Theory of enhanced second-harmonic generation by the quadrupole–dipole hybrid exciton

2008 J. Phys.: Condens. Matter 20 235238

(http://iopscience.iop.org/0953-8984/20/23/235238)

IOP PUBLISHING JOURNAL OF PHYSICS: CONDENSED MATTER

J. Phys.: Condens. Matter **20** (2008) 235238 (9pp) doi:10.1088/0953-8984/20/23/235238

Theory of enhanced second-harmonic generation by the quadrupole–dipole hybrid exciton

Oleksiy Roslyak and Joseph L Birman

Physics Department, The City College, CUNY, Convent Avenue at 138 Street, New York, NY 10031, USA

E-mail: avroslyak@gmail.com

Received 27 November 2007, in final form 2 April 2008
Published 13 May 2008
Online at stacks.iop.org/JPhysCM/20/235238

Abstract

We report calculated substantial enhancement of the second-harmonic generation (SHG) in cuprous oxide crystals, resonantly hybridized with an appropriate organic material (DCM2:CA:PS 'solid state solvent'). The quadrupole origin of the inorganic part of the quadrupole–dipole hybrid provides inversion symmetry breaking and the organic part contributes to the oscillator strength of the hybrid. We show that the enhancement of the SHG, compared to the bulk cuprous oxide crystal, is proportional to the ratio of the DCM2 dipole moment and the effective dipole moment of the quadrupole transitions in the cuprous oxide. It is also inversely proportional to the line-width of the hybrid and bulk excitons. The enhancement may be regulated by adjusting the organic blend (mutual concentration of the DCM2 and CA part of the solvent) and pumping conditions (varying the angle of incidence in the case of optical pumping or populating the minimum of the lower branch of the hybrid in the case of electrical pumping).

1. Introduction

Considerable attention has been paid to the relatively strong optical second-harmonic generation (SHG) in thin film (D_{4h} symmetry) and bulk (O_h symmetry) cuprous oxide crystals. This was first addressed in the pioneering work of Shen *et al* (1996). The effect is attributed to the electric-quadrupole $\hbar\omega_{1S} = 2.05$ eV exciton effect. The quadrupole exciton has very small oscillator strength but it possess rather narrow line-width $\hbar\gamma_{1S}$ so the effect is well pronounced when the exciting laser energy is close to one $\hbar\omega_{1S} - \hbar\omega \ll \hbar\gamma_{1S}$ or two photon resonance $\hbar\omega_{1S} - 2\hbar\omega \ll \hbar\gamma_{1S}$. In the dipole approximation this effect disappears (Atanasov *et al* 1994).

We propose to amplify the SHG characteristic of the $1S$ quadrupole Wannier exciton (WE) in cuprous oxide by making a hybrid with an organic Frenkel exciton (FE) (see the next section for more details). The idea of resonant enhancement of some nonlinear properties generic to semiconductor dipole-allowed Wannier–Mott (WE) excitons was presented in the pioneering work of Agranovich *et al* (1998) for layered organic–inorganic heterostructures. It was also developed for quantum wires and dots embedded into an organic shell (Engelmann *et al* 1998, Gao *et al* 2004) or attached to dendrimer structure (Huong and Birman 2000, 2003).

In our previous work (Roslyak and Birman 2007a) we demonstrated considerable enhancement of another nonlinear effect in cuprous oxide, photo-thermal bi-stability which was measured in pure Cu_2O crystals (Dasbach 2004). We demonstrated a considerable enhancement in the hysteresis-like region size (from μeV for bulk cuprous oxide to meV for the hybrid). The enhancement was attributed to the large oscillator strength of the hybrid exciton inherited from the organic part and the still rather narrow line-width, of the same order as the coupling. Analogous enhancements can be expected for the SHG, which is the subject of this paper.

In section 2 we propose a pump–probe experiment to reveal the SHG enhancement due to the resonant dynamical hybridization and briefly discuss relevant quadrupole hybrid exciton properties. In section 3 we address the question of how this resonant[1] enhancement depends on such parameters of the system as oscillator strengths and damping of the FE and WE constituting the hybrid. Using a classical model of nonlinear

[1] The resonance occurs between the FE and WE energies.

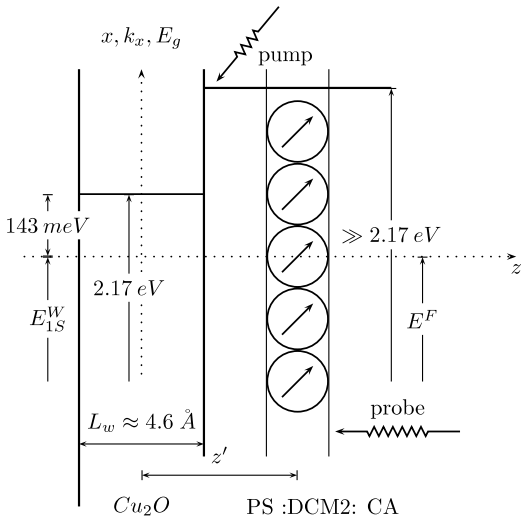

Figure 1. Schematic representation and the energy offset of a possible experimental set-up to observe the enhanced SHG by the quadrupole–dipole exciton. Here the inorganic Cu_2O quantum well provides the $1S$ quadrupole WE. The DCM2 part of the organic 'solid state solute' provides dipole-allowed FE (set of small arrows); the PS host prevents wavefunction overlapping between organic and inorganic excitons; CA under proper concentration allows tuning of the excitons into the resonance.

coupled oscillators, we demonstrate that while the large ratio of the hybrid oscillator strength suggests many orders of magnitude enhancement it is actually somehow reduced by the rather small coupling parameter and density of the FE.

Because the FE is dynamically brought into resonance with the WE there is an important hybridization time τ_h parameter. Hence, in section 4, we develop a more sophisticated quantum mechanical model to address the dynamics of the hybrid SHG. Namely we show that the signal enhancement drastically depends on whether one probes the system before or after the hybridization occurred.

2. Proposed experimental set-up for the SHG

In this work we adopt the concept of a layered organic–inorganic heterostructure. The inorganic component of the hybrid is a thin layer of Cu_2O (quantum well, latter in the text referred to as QW) grown upon a film of the organic composite (see figure 1). Due to the small radius of both the WE and FE exciton part of the hybrid one can neglect the effect of confinement. In this case one cannot tune the two types of excitons in resonance by adjusting the confinement ($L_w > a_B^W \approx$ to the cuprous oxide unit cell $a = 4.6$ Å). The QW confinement just assures that the WE propagates along the interface and is subjected to the electric field gradient of the FE propagating along the adjacent chain of the DCM2 molecules.

To provide resonance between WE in cuprous oxide and FE in the organic, we propose utilization of 'solid state solvation' (SSS) of the DCM2 molecules[2] in a transparent polystyrene (PS) host doped with camorphic anhydride (CA) (Bulovic *et al* 1999). The SSS is a type of solvatochromism manifesting itself as a change in the spectral position of the absorption/luminescence band due to change in the polarity of the medium. The Förster dipole–dipole non-resonant interaction between DCM2 and CA modifies the energy structure of the molecules involved.

During the 'slow' phase ($\tau_s \approx 3.3$ ns) the energy of the FE experiences[3] a red shift linear with the CA concentration due to a non-resonant dipole–dipole interaction with the CA molecules. Note that our model capitalizes on the fact that DCM2 molecules form a 2D layer rather than being diluted in the PS:CA solvent which is the case for currently manufactured optical light emitting devices (OLED). This allows us to neglect the rather complicated problem of the inhomogeneous broadening of the FE energy by utilizing a *mean field* approximation[4]. For the mean field approximation the red spectral shift of the FE energy in resonance with the quadrupole WE can be accomplished with $\rho_{CA} \approx 22\%$ CA concentration.

To avoid complicated problems of time dependent hybridization and stay within the analytical model framework, we assume that the FE and WE are in exact resonance once the DCM2 energy is in close proximity to the WE energy i.e. $\hbar\omega_{DCM2} - \hbar\omega_{1S} \leqslant \Gamma_k$. We introduced the quadrupole–dipole coupling parameter $\Gamma_k \leqslant 4\ \mu$eV (Roslyak and Birman 2007b) (see also appendix (A.1)). This resonant coupling gives rise to the upper and lower branches of the quadrupole–dipole hybrid (QDH) dispersion[5]: $\hbar\omega_{u,l} = \hbar\omega_{1S} \pm \Gamma_{\mathbf{k}}$. To populate both of the branches one needs a second pumping photon tuned into resonance with the $1S$ transition.

The radiation field interacts through both dipole and quadrupole parts of the hybrid. The dipole interaction can be used to produce a linear response signal due to the pumping (Roslyak and Birman 2007a). By using the nonlinear response to the probe signal, the second harmonic can be generated through the quadrupole part of the hybrid. Different SHG regimes can be achieved by changing the timing between pumping and probe signals (see section 4 for more details).

According to the selection rules for the quadrupole–dipole hybrid, the pumping signal, running along the organic–inorganic interface of the heterostructure, induces a linear polarization in the z direction (Roslyak and Birman 2007b). The probe signal induces a second order nonlinear response in the cuprous oxide. This is perpendicular to the interface, and defined by the second order polarization along the x direction (see figure 1). The net polarization is given by a second rank tensor through the following expression:

$$P_z^{(1)} + P^{(2)}_{l=\hat{j}\times\hat{x}} = \chi^{(1)}_{i,z} E_i + \mathrm{i}\chi^{(2)}_{l,i,j,x} k_x E_i E_j. \qquad (1)$$

Here E_i, E_j are the electric field of the pumping and probe lasers correspondingly. The x component of the probe

[2] [2-methyl-6-2-(2,3,6,7-tetrahydro-1H, 5H-benzo[i,j]-quinolizin-9-yl)-ethenyl]-4H-pyran-4-ylidene] propane dinitritle.

[3] In our case we define the FE as DCM2 excitation.

[4] Indeed, in our simplified model the DCM2 molecules are not randomly situated but rather form a uniform (homogeneous) thin layer near the interface. Also the experimentally observed FE energy relaxation shows no significant energy fluctuations. These experiments have been performed at MIT by Dr Bulovic. The results are not officially published yet, but have been reported in the MIT proceedings.

[5] See the eigenvalues of the linearized system (4) or the Hamiltonian (8).

signal wavevector is taken to be close to zero to avoid possible interference in momentum conservation. For the sake of simplicity we are going to omit x and l indexes of the tensor keeping in mind that the wavevector of the pump signal has only an x component and the SH signal is perpendicular to it and the probe signal polarization: $i\chi^{(2)}_{l,i,j,x}k_x = \chi^{(2)}_{i,j}$.

In this paper we develop both classical and quantum mechanical models, which can be used to find a specific form of the hybrid second order nonlinear susceptibility. In section 3 we demonstrate that the second order nonlinearity (generic to the cuprous oxide and introduced through a small parameter λ) is enhanced due to the resonant quadrupole–dipole hybridization with the organic (see (5)). In section 4 we develop the quantum theory of the enhanced SHG. It allows the investigation of different regimes of the process defined by the time ordering between the probe pulse and the time when the FE and WE energies are close enough to form the hybrid. We generalize the concept of the double-sided Feynman diagrams (Mukamel 1995) to include non-radiative processes for the energy exchange between DCM2 and CA as well as resonant QDH between DCM2 and cuprous oxide.

3. Anharmonic coupled oscillators model

As a first step, we will use the simplest classical model neglecting the non-local effects of the linear $\chi^{(1)}_{i,z}$ and nonlinear susceptibility $\chi^{(2)}_{l,i,j,x}$ to describe the hybrid SHG. Namely, we adopt an extension of the anharmonic oscillator model (Bloembergen 1965, Mukamel 1995) generalized for the case of resonant coupling between two distinct sets of oscillators. This simplified picture only covers the case when the pumping field is polarized along $\hat{z} \parallel [001]$ axis ($E_i = E_z$) and we probe the hybrid system ($\omega_{1S} = \omega_F$) with a signal perpendicular to the interface and polarized along $\hat{y} \parallel [010]$ direction ($E_j = E_y$).

We consider the WE in cuprous oxide as an assembly of oscillators with the oscillator strength per unit cell given by $f_{xz,k} \propto k_x$ (see for example Moskalenko and Liberman (2002)). The second set of the oscillators with the oscillator strength given by f^{F} corresponds to the FE in the organic.

Treating the wavevector k as just another parameter[6], the polarization P^{W}, P^{F} due to WE and FE can be written in terms of the effective electron–hole displacements X, Y as:

$$P^{\mathrm{W}} = \frac{N}{a_{\mathrm{B}}^{\mathrm{W}} S} f_{xz,k} e X \tag{2}$$

$$P^{\mathrm{F}} = \frac{\rho_{\mathrm{DCM2}} N}{a_{\mathrm{B}}^{\mathrm{F}} S} f^{\mathrm{F}} e Y. \tag{3}$$

[6] In the text we are going to omit the index k unless we put an emphasis on it.

Here S is the area of the interface and $a_{\mathrm{B}}^{\mathrm{W}}, a_{\mathrm{B}}^{\mathrm{F}}$ are the WE and FE Bohr radius, e is the electron charge. The surface density of the WE and FE excitons are $N f_{xz,k}/(a_{\mathrm{B}} S)$ and $\rho_{\mathrm{DCM2}} N f^{\mathrm{F}}/(a_{\mathrm{B}} S)$ correspondingly and N is the total number of the oscillators. Here we also took into account the low density ($\rho_{\mathrm{DCM2}} = 0.05\%$) of the DCM2 molecules in the organic to avoid the aggregation effect (Madigan and Bulovic 2003).

In the time frame of the hybridization $\tau_{\mathrm{s}} - \tau_{\mathrm{h}} < t < \tau_{\mathrm{s}}$, the WE and FE energies are at perfect resonance. Hence, the system of equations governing the oscillator dynamics can be written in the form:

$$\begin{aligned} \ddot{X} + \omega_{1S}^2 X + \gamma \dot{X} - \frac{2\omega_{1S}\Gamma_k}{\hbar} Y - \omega_{1S}^2 \lambda X^2 = 0 \\ \ddot{Y} + \omega_{1S}^2 Y + \gamma \dot{Y} - \frac{2\omega_{1S}\Gamma_k}{\hbar} X = \frac{e}{m} E_i \mathrm{e}^{\mathrm{i}\omega t}. \end{aligned} \tag{4}$$

The nonlinear factor $\omega_{1S}^2\lambda$ appears due to the probe signal. It is defined such that λ has dimensions of reciprocal length and is considered to be small in the sense that it is much less than the reciprocal of the maximum displacement of the FE (Y) and WE (X) oscillators. The exact value of λ can be obtained either from an experiment or from the microscopic quantum theory (see the next section for more details).

The terms proportional to γ describe the QDH damping. The terms proportional to $2\omega_{1S}\Gamma_k/\hbar$ describe the quadrupole–dipole coupling. Hence, the eigenvalues of the linearized system of equations (4) give both branches of the QDH.

The system is driven dominantly by the light–dipole interaction in the organic and the quadrupole–light interaction is neglected (m is the electron mass).

Using standard perturbation theory with respect to the small parameter λ in zero order (neglecting the quadratic term) and combining equations (1), (2) and (4) one has the linear response of the hybrid and bulk cuprous oxide given by the following expressions:

$$\chi^{(1)}_{\mathrm{Hy}}(\omega) = \frac{\rho_{\mathrm{DCM2}} N}{a_{\mathrm{B}}^{\mathrm{F}} S} \frac{f^{\mathrm{F}} e^2/m(\omega_{1S}^2 - \omega^2 + \mathrm{i}\omega\gamma)}{(\omega_{1S}^2 - \omega^2 + \mathrm{i}\omega\gamma)^2 - (2\omega_{1S}\Gamma_k/\hbar)^2}$$

$$\chi^{(1)}_{\mathrm{Cu_2O}}(\omega) = \frac{N}{a_{\mathrm{B}}^{\mathrm{W}} S} \frac{f_{xz,k} e^2/m}{\omega_{1S}^2 - \omega^2 + \mathrm{i}\gamma}.$$

Including the nonlinear term as a source for the SHG to first order in the perturbation parameter, there is a displacement at 2ω. The SHG response is given by a solution of the following coupled system:

$$\begin{aligned} \ddot{X} + \omega_{1S}^2 X + \gamma \dot{X} - \frac{2\omega_{1S}\Gamma_k}{\hbar} Y - \omega_{1S}^2 \lambda X_{\lambda=0}^2 = 0 \\ \ddot{Y} + \omega_{1S}^2 Y + \gamma \dot{Y} - \frac{2\omega_{1S}\Gamma_k}{\hbar} X = 0. \end{aligned}$$

Using the definitions (1) and (2) one gets the following nonlinear second order response function for the hybrid and

bulk cuprous oxide correspondingly:

$$\chi^{(2)}_{\mathrm{Hy}}(2\omega;\omega,\omega) = \frac{\rho_{\mathrm{DCM2}}N}{a_{\mathrm{B}}^{\mathrm{F}}S} \times \frac{f^{\mathrm{F}}e^3/m^2\omega_{1S}^2\lambda(2\omega_{1S}\Gamma_k/\hbar)}{((\omega_{1S}^2-(2\omega)^2+\mathrm{i}2\omega\gamma)^2-(2\omega_{1S}\Gamma_k/\hbar)^2)^2} \times \frac{(\omega_{1S}^2-\omega^2+\mathrm{i}\omega\gamma)^2}{(\omega_{1S}^2-\omega^2+\mathrm{i}\omega\gamma)^2-(2\omega_{1S}\Gamma_k/\hbar)^2} \quad (5)$$

$$\chi^{(2)}_{\mathrm{Cu_2O}}(2\omega;\omega,\omega) = \frac{N}{a_{\mathrm{B}}^{\mathrm{W}}S}\frac{f_{xz,k}e^3/m^2\omega_{1S}^2\lambda}{(\omega_{1S}^2-(2\omega)^2+\mathrm{i}2\gamma)(\omega_{1S}^2-\omega^2+\mathrm{i}\gamma)^2}.$$

Straightforward comparison of the expressions above evinces the resonant rise of the second order nonlinearity owing to hybridization. There are several competing factors involved. The enhancement by means of large oscillator strength ratio $f^{\mathrm{F}}/f_{xz,k}$ is reduced by the rather small coupling parameter Γ_k and small DCM2 density ρ_{DCM2} (see more numerical details in section 5).

4. Quantum theory of SHG due to the QDH

Although the system of nonlinear susceptibilities (5) in principle solves the problem of SHG due to the hybrid it does not clarify the origin of the nonlinearity λ. Also, such an important parameter as the hybridization time τ_{h} is left out of the classical description. Hence, in this section we propose a unified quantum theory of the hybrid SHG.

The linear response of the hybrid is due to dipole transitions from the ground $|g\rangle$ state[7] to the FE $|F\rangle$ in the organic and due to quadrupole transitions to the WE $|1S\rangle$ in the cuprous oxide. The nonlinearities are the result of some intermediate inter-band transitions in the cuprous oxide (Mukamel 1995).

In cuprous oxide the nearest state in energy to the quadrupole ortho-exciton $\hbar\omega_{1S}(\Gamma_5^+)$ is the $\hbar\omega_{2P}(\Gamma_4^-)$ dipole-allowed excitonic band $|2P\rangle$, $E_{\mathrm{g}} > \hbar\omega_{2P} > \hbar\omega_F > \hbar\omega_{1S}$. Hence it plays the main role in formation of the nonlinear response and can be excited by a properly tuned probe signal. We neglect the remaining inter-band and intra-band[8] transitions. Therefore, the states above form a complete basis for the SHG problem:

$$|g\rangle, |1S\rangle, |F\rangle, |2P\rangle. \quad (6)$$

Inversion symmetry of the DCM2 is also broken by the CA induced local field and the interface effect. Therefore, unlike in the classical model, the contribution from the organic to the SHG has to be considered as well. But due to the smallness of the symmetry breaking local field it only contributes a little to the SHG enhancement.

Using the basis above let us introduce creation operators for the FE and the $1S$ and the $2P$ WE exciton $b^\dagger = |F\rangle\langle g|$, $B_{1S}^\dagger = |1S\rangle\langle g|$, $B_{2P}^\dagger = |2P\rangle\langle g|$ respectively. The commutation algebra of the operators is presented in the appendix (B.1).

The net polarization of the sample is defined as (Mukamel 1995):

$$P = \mu^i_{1S,k}(B^\dagger_{1S}+B_{1S}) + \mu^i_{2P}(B^\dagger_{2P}+B_{2P}) + \mu^i_F(b^\dagger+b) + \mu^j_{1S,2P}(B^\dagger_{1S}B_{2P}+B_{1S}B^\dagger_{2P}). \quad (7)$$

Here $\mu^i_{1S,k} = \hat{i}\cdot\hat{z}k_xQ_{x,z} = 3\times10^{-5}(k_x/k_{0,x})D$ is an effective dipole moment (Moskalenko and Liberman 2002, Roslyak and Birman 2007b) due to the quadrupole transitions associated with the oscillator strength; k_0 is the resonant wavevector for bulk cuprous oxide (appendix (A.2)). The dipole moment of the transitions from $|1S\rangle$ to $\langle 2P|$ is defined by (Artoni *et al* 2002, Elliott 1961):

$$\left(\mu^j_{1S,2P}\right)^2 = \frac{Ne^2\hbar^2f_{2P}}{Sa_{\mathrm{B}}^{\mathrm{W}}2m^\star E_{2P}}\left(\hat{j}\times\hat{x}\right)^2 = 6\times10^{-3}D^2.$$

Finally, the DCM2 dipole moment of the transition from $|g\rangle$ to $\langle F|$ per unit area of the interface is given by (Madigan and Bulovic 2004):

$$(\mu^i_F)^2 = \frac{\rho_{\mathrm{DCM2}}Ne^2\hbar^2f^{\mathrm{F}}}{Sa_{\mathrm{B}}^{\mathrm{F}}2m^*\hbar\omega_{1S}} = 0.2D^2.$$

Using equation (7) and the rotating wave approximation for the resonant wavevector k, the hybrid Hamiltonian can be written as:

$$H = \hbar\omega_Fb^\dagger b + \hbar\omega_{1S}B^\dagger_{1S}B_{1S} + E_{2P}B^\dagger_{2P}B_{2P} + \Gamma_k\left(B^\dagger_{1S}b + B_{1S}b^\dagger\right) + \mu^i_F\left(b^\dagger E^\dagger_i + bE_i\right) + \mu^i_{1S,k}\left(B^\dagger_{1S}E^\dagger_i + B_{1S}E_i\right) + \mu^i_{2P}\left(B^\dagger_{2P}E^\dagger_i + B_{2P}E_i\right) + \mu^j_{1S,2P}\left(B^\dagger_{1S}B_{2P}E^\dagger_j + B_{1S}B^\dagger_{2P}E_j\right). \quad (8)$$

The linear response from *both* branches of the hybrid may be observed by pumping the hybrid with two signals $E_i \parallel \hat{z} \propto \mathrm{e}^{\mathrm{i}\omega t}$. The first photon $\hbar\omega = E_{\mathrm{DCM2}}$ excites DCM2 molecules. During the time period $\tau_{\mathrm{s}}-\tau_{\mathrm{h}}$ the system relaxes to the FE exciton energy close to $\hbar\omega_{1S}$ thus providing resonance between WE and FE. Then the second pumping photon $\hbar\omega = \hbar\omega_{1S}$ enters and excites the quadrupole WE so that both QDH branches are populated. The QDH exciton lives for τ_{h} nanoseconds and then both branches of the hybrid relax to the ground state, emitting photons of energy $\hbar\omega_{1S}\pm\Gamma_k$.

Generalizing conventional double-sided Feynman diagrams (Mukamel 1995) to include the non-radiative processes, the linear response from the QDH can be represented by the following diagram:

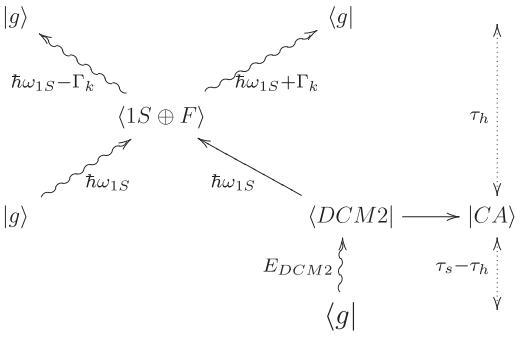

(9)

[7] When no excitations are present in the system.

[8] Due to the small radius of the quadrupole WE.

$$\chi_i^{(1)}(\omega,k)=\mu^i_{1S,0}(B^\dagger_{1S,0}+B_{1S,0})+\mu^i_F(b_0^\dagger+b_0)$$
$$=\frac{(\mu^i_F)^2(\hbar\omega-\hbar\omega_{1S}+\mathrm{i}\hbar\gamma)+\mu^i_F\mu^i_{1S}\Gamma_k}{(\hbar\omega-\hbar\omega_{1S}+\mathrm{i}\hbar\gamma)^2-\Gamma_k^2}+\text{c.c.} \qquad (10)$$

On the diagram the wavy lines represent the incoming and outgoing photons; the straight lines stand for the non-radiative transitions. The diagram shows energy exchange between photon–exciton and exciton–exciton as well as the time separation between two pumping signals. Time increases from bottom to the top of the diagram as for the conventional Feynman diagram. The hybrid lifetime is denoted as $\tau_\mathrm{h}=1/\gamma$ and the hybridization between FE and WE is denoted as $\oplus$.

In the derivation of the linear response $\chi_i^{(1)}(\omega,k)$ we used equation (7) along with solutions of the Heisenberg equations of motion presented in the appendix B (B.2). Formally the linear response can be written in terms of the hybrid Green's functions as:

$$\chi_i^{(1)}(\omega,k)=\sum_{a,b=\{g,1S,F\}}\mu^i_{ab}\mu^i_{ba}I_{ab}(\omega)$$
$$I_{1S,g}=I_{F,g}=\frac{\hbar\omega-\hbar\omega_{1S}+\mathrm{i}\hbar\gamma}{(\hbar\omega-\hbar\omega_{1S}+\mathrm{i}\hbar\gamma)^2-\Gamma_k^2}$$
$$I_{1S,F}=\frac{\Gamma_k}{(\hbar\omega-\hbar\omega_{1S}+\mathrm{i}\hbar\gamma)^2-\Gamma_k^2}$$
$$I_{ab}=I^\star_{ba}.$$

Here the dipole matrix elements in the corresponding basis (6) are given by:

$$\begin{pmatrix}0&\mu_{1S}&\mu_F&0\\ \mu_{1S}&0&\sqrt{\mu_{1S}\mu_F}&0\\ \mu_F&\sqrt{\mu_F\mu_{1S}}&0&0\\ 0&0&0&0\end{pmatrix}.$$

Note that we neglected the non-resonant term associated with ground state dipole moment of the organic μ_g.

The SHG is due to second order response $E_j\perp E_i\parallel z$ and given by the last term in equation (7) and the solutions of the equations of motion (B.2), (B.3). The first type of SHG is formed when the branches of the hybrid interacts with the $|2P\rangle$ level excited by the probe signal. Using all the diagram conventions we adopted above, the diagram for this nonlinear process is given below:

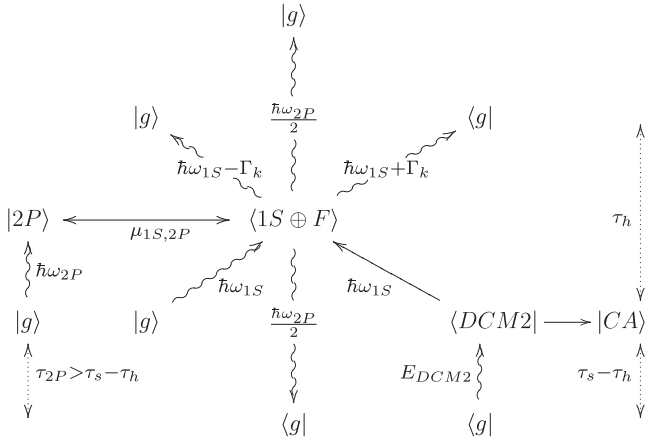

(11)

$$\chi^{(2)}_{ij}(2\omega;\omega,\omega)=\mu_{1S,2P}\left(B^\dagger_{1S,0}B_{2P,1}+\text{c.c.}\right)$$
$$=\frac{\mu^i_{2P}\mu^j_{1S,2P}\left(\mu^i_{1S}(\hbar\omega-\hbar\omega_{1S}+\mathrm{i}\hbar\gamma)+\mu^i_F\Gamma_k\right)}{(2\hbar\omega-\hbar\omega_{2P})\left((\hbar\omega-\hbar\omega_{1S}+\mathrm{i}\hbar\gamma)^2-\Gamma_k^2\right)}+\text{c.c.} \qquad (12)$$

Here the probe signal comes *after* the hybrid is formed: $\tau_{2P}>\tau_\mathrm{s}-\tau_\mathrm{h}$.

Another second order nonlinear response can be formed if the probe signal comes *before* the hybridization $\tau_{2P}<\tau_\mathrm{s}-\tau_\mathrm{h}$. It can be represented by the following diagram:

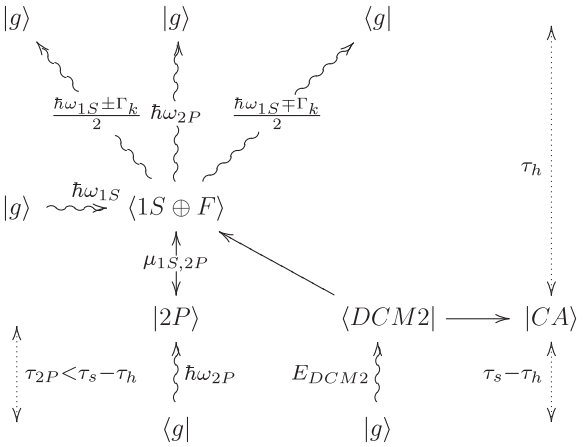

$$\chi^{(2)}_{ij}(2\omega;\omega,\omega)=\mu_{1S,2P}(B^\dagger_{1S,1}B_{2P,0}+\text{c.c.})$$
$$=\frac{\mu^i_{2P}\mu^j_{1S,2P}(\mu^i_{1S}(2\hbar\omega-\hbar\omega_{1S}+\mathrm{i}\hbar\gamma)+\mu^i_F\Gamma_k)}{(\hbar\omega-\hbar\omega_{2P})((2\hbar\omega-\hbar\omega_{1S}+\mathrm{i}\hbar\gamma)^2-\Gamma_k^2)}.$$

The Green's function representation of the SHG due to the second order response is given by the following expression:

$$\chi^{(2)}_{ij}(2\omega;\omega,\omega)=\mu^j_{1S,2P}\sum_{a=\{g,1S,F,2P\}}\mu^i_{a,1S}\mu^i_{2P,a}$$
$$\times\left[I_{a,1S}(\omega)\,I_{a,2P}(2\omega)+I_{1S,a}(2\omega)\,I_{2P,a}(\omega)\right]$$
$$I_{2P,g}=\frac{1}{\hbar\omega-\hbar\omega_{2P}}.$$

The dipole matrix elements on the basis (6) are given by:

$$\begin{pmatrix}0&\mu_{1S}&\mu_F&\mu_{2P}\\ \mu_{1S}&0&\sqrt{\mu_{1S}\mu_F}&\mu_{1S,2P}\\ \mu_F&\sqrt{\mu_F\mu_{1S}}&0&0\\ \mu_{2P}&\mu_{1S,2P}&0&0\end{pmatrix}.$$

According to the last term in the equation (7), the signal at $2\hbar\omega=\hbar\omega_{1S}\pm\Gamma_k$ may generate a signal at $\hbar\omega=\hbar\omega_{1S}\pm\Gamma_k$:

$$\chi^{(3)}_{ij}(\omega;2\omega,-\omega)$$
$$=\frac{\mu^i_{2P}(\mu^j_{1S,2P})^2(2\hbar\omega-\hbar\omega_{1S}+\mathrm{i}\hbar\gamma)}{(\hbar\omega-\hbar\omega_{2P})^2((2\hbar\omega-\hbar\omega_{1S}+\mathrm{i}\hbar\gamma)^2-\Gamma_k^2)}+\text{c.c.}$$

This type of signal has been experimentally detected (Shen *et al* 1996) in bulk cuprous oxide ($\Gamma_k=0$) when the pumping signal was tuned to the wavelength between 12 285 and 12 195 Å. A strong SH signal was detected at 6096 Å which has to be attributed not only to the narrow line-width of the quadrupole exciton but to the fact that $\mu_{1S,2P}\gg\mu_{1S}$ as well. From the last expression it follows that in this case no

increment in the outgoing signal can be expected due to the hybridization effect.

The third order nonlinearity is responsible as well for some small contribution to the SHG due to the non-zero ground state dipole moment of the DCM2 molecules (Kishida *et al* 1994). In the local electric field created by the polar CA molecules on the interface $E_{\rm loc}(0)$, the SH signal is due to the third order susceptibility $\chi^{(3)}_{ij}(2\omega;\omega,\omega,0)$. The exact expression in terms of the corresponding Green's functions is too lengthy to be listed here (Mukamel 1995), therefore we provide numerical calculations of the total SHG including the above correction in the next section.

5. Results and discussion

In order to make a numerical comparison of the hybrid and bulk SHG the lifetime of the hybrid plays a major role. Considering the bi-stability effect in the hybrid (Roslyak and Birman 2007a) we assumed that the cuprous oxide has purity of 99.99% with the reported line-width of $\hbar\gamma_{1S} = 0.1$ meV (picosecond lifetime) (Shen *et al* 1996). Therefore the hybrid lifetime is dominated by its inorganic part $\hbar\gamma \approx \hbar\gamma_{1S}$. To compensate for such a large line-width we also assumed that the DCM2 is presented as a thin film embedded into PS host close to the interface with the cuprous oxide. For the nonlinear absorption experiment this assumption can be justified as it makes the absorption length of the hybrid equal to the narrow region around the interface, of the size of the hybrid itself. However, there is a drawback in that model due to possible aggregation of the DCM2.

Hence in this paper we adopted the picture of a disordered organic and higher purity of the inorganic crystal. This will bring the line-width and the coupling parameter to the same order. For pure cuprous oxide crystal the lifetime of the quadrupole $1S$ exciton is reported to be $\tau_{1S} = 1.7\ldots3.0$ ns ($\hbar\gamma = 1\ldots0.5$ μeV) (Dasbach 2004, Frohlich *et al* 2005, Elliott 1961). Such higher purity crystals and thin films are widely used in searching for BEC of excitons.

In this case the lifetime of the $1S$ quadrupole exciton is mainly determined by the ortho–para exciton conversion. The lifetime of the organic part of the hybrid is determined by the time the excited DCM2 molecule takes to reach an equilibrium with the bath of polar CA molecules. The lifetime for the given concentration of the CA is reported to be 3.3 ns (Madigan and Bulovic 2003, 2004). Because these processes are of the same order, the effective lifetime of the hybrid is a non-trivial combination of the effects described above and will be reported elsewhere. Here we assume the simplest case of a non-coherent lifetime of the hybrid $\hbar\gamma = 0.29$ μeV (Roslyak and Birman 2007b).

The intensity of the second harmonic is proportional to $|\chi^{(2)}k_x|^2$ (see for example (Haueisen and Mahr 1973)). Therefore an important measurable quantity is the relative value of nonlinear susceptibility $|\chi^{(2)}k_x|$ presented in figure 2.

The SHG signal is split according to the response from the lower and upper branch of the hybrid. Asymmetry between these two branches is a result of quantum effects and not present in the classical anharmonic oscillator picture. We also included the corrections due to the interface effect in the organic in our numerical simulation.

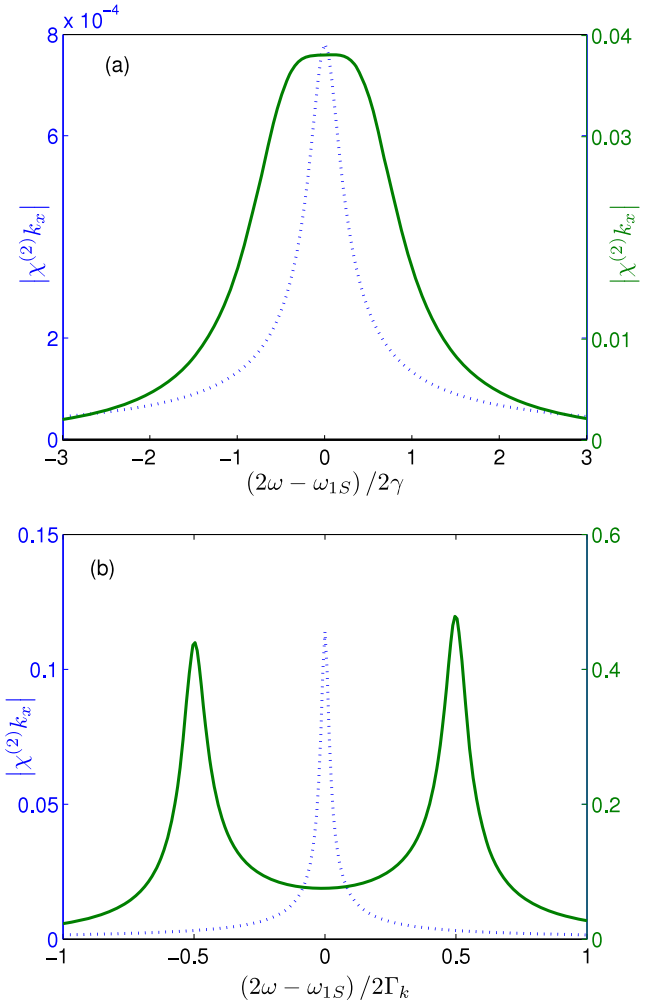

Figure 2. Relative value of the nonlinear susceptibility in the case of bulk cuprous oxide (dotted curves) and the quadrupole–dipole hybrid (solid curves). The density of the disordered DCM2 is taken as $\rho_{\rm DCM2} = 0.005\%$ while the CA density is $\rho_{\rm CA} = 22\%$. The (a) represents moderate coupling $\Gamma_k = \hbar\gamma_{1S} = 0.29$ μeV and (b) corresponds to the strong coupling regime $\Gamma_k = 3.5$ μeV. In the last case the enhancement is evident and indicated by the different scales for the bare cuprous oxide (left) and hybrid (right) SHG

(This figure is in colour only in the electronic version)

For the sake of simplicity let us consider two distinct cases. First, the pump laser is perpendicular to the interface. The states up to $ka = k_0a$ are populated thermally. No hybridization occurs and it is equivalent to the bulk case SHG (see figure 2 dotted curve). The maximum power generated by the second harmonic is proportional to the square of the following expression:

$$|\chi^{(2)}_{ij,\max}(2\hbar\omega = \hbar\omega_{1S})| = \frac{\mu_{2P}\mu_{1S,2P}}{\hbar\omega - \hbar\omega_{2P}}\frac{\mu_{1S,k}k_x}{\hbar\gamma_{1S}}. \qquad (13)$$

The small relative value of the SHG is due to the narrowness of the cuprous oxide quantum well.

Second, the pump laser incidence angle is reduced to acquire the wavevector $k_0 a \ll ka$. The maximum power generated by the second harmonic is proportional to the square of the following expression:

$$|\chi^{(2)}_{ij,\max}(2\hbar\omega = \hbar\omega_{1S} \pm \Gamma_k)| = \frac{\mu_{2P}\mu_{1S,2P}}{\hbar\omega - \hbar\omega_{2P}} \frac{\mu_F k_x}{\alpha_k \hbar\gamma}. \quad (14)$$

Here the incidence angle dependent coefficient $\alpha_k = \sqrt{5}$ (see figure 2(a)) for $ka = 0.13$ ($\Gamma_k = \hbar\gamma = 0.29$ μeV) and $\alpha_k = 2$ for the maximum value of the coupling $\Gamma_k = 3.5$ μeV at $ka = 1.57$ (see figure 2(b)). Finally, comparing the last expression (14) to that for bulk cuprous oxide (13) the second order response of the hybrid is amplified by the factor:

$$\left(\frac{\mu_F}{\mu_{1S}} \frac{\hbar\gamma_{1S}}{\alpha\hbar\gamma}\right)^2.$$

Therefore the amplification can be adjusted by manipulating the organic composition (DCM2 and CA densities) or changing the pump laser incidence angle.

Finally, we would like to note that there is another merit in using a hybrid structure for the SHG. Namely the fact that optical pumping can be replaced by electrical pumping. For this, the hybrid sample has to be placed between Alq3 and a-NPD (Madigan and Bulovic 2004) semiconductor plates. The bond structure and offset of these materials provide electrons and holes to form the hybrid exciton on the interface. Although, in this case, one can expect the SHG only from the lower branch of the hybrid as the excitons are accumulated at the minimum of the hybrid dispersion (Roslyak and Birman 2007b).

6. Conclusion

In this paper we addressed the possibility of enhancing the SHG signal $\chi^{(2)}$ generic to a cuprous oxide bulk crystal as the lowest excitation in this material has a quadrupole origin. To demonstrate the concept we proposed considering a pump–probe experiment performed on cuprous oxide sandwiched between the organic composite. An intense pump signal excites one part of the organic known as DCM2 (FE). Non-resonant (Förster) energy transfer in the organic layer ('solid state solvation' effect) provides a dynamical red shift of the FE. When the FE energy is close enough to the quadrupole-allowed $1S$ exciton in the adjacent cuprous oxide the quadrupole–dipole hybridization occurs due to the FE induced gradient of the electric field penetrating into the inorganic layer. The probe signal is designed to reveal the SHG signal.

The resonant enhancement of the $\chi^{(2)}$ occurs because the hybrid exciton shares properties of both quadrupole WE (long radiative lifetime) and organic FE (big oscillator strength). Its quadrupole part allows $\chi^{(2)}$ to be non-vanishing, while its FE part provides the enhancement of the SHG signal compared to the bare cuprous oxide crystal due to more efficient absorption of the pump signal by means of the large oscillator strength of the hybrid.

However, as we demonstrated in the classical coupled oscillator model framework,the enhancement is determined not only by the large ratio of the corresponding organic/inorganic oscillator strengths but somehow quenched by the small coupling parameter and low DCM2 density. By varying those parameters the hybrid SHG signal may be enhanced by orders of magnitude compared with the generic (cuprous oxide) one.

To reveal the enhancement dependence on such an important parameter of the hybrid as the hybridization time τ_h we investigated a more sophisticated quantum theory. It suggests that there is substantial difference in the hybrid SHG signal provided one probes the system before or after the hybridization occurred. In the first case the SH is generated at $\omega_{2P}/2$ frequency. Hence it is vastly suppressed by the short lifetime of the dipole-allowed 2P WE in cuprous oxide. Nevertheless, if one probes the system after the hybridization has happened, the SH is generated at $\omega_{1S}/2$ and is heightened by the large oscillator strength of the hybrid and its small damping coefficient.

Acknowledgments

We would like to thank Ms Upali Aparajita for helpful discussion and comments. The project was supported in part by PCS-CUNY.

Appendix A

An explicit expression for the quadrupole–dipole coupling is given below:

$$\Gamma_k = \frac{8\sqrt{2\pi}}{(\varepsilon + \tilde{\varepsilon})\, L_w} \frac{k e^{-kz'} \sinh\left(\frac{L_w k}{2}\right)}{\left(1 + \left(\frac{kL_w}{2\pi}\right)^2\right)} \frac{Q_{xz}\mu_z^F}{a_B^F a_B^W L_w}. \quad (A.1)$$

Here a_B^F, a_B^W are the Bohr radii of the FE and WE exciton; $\tilde{\varepsilon}$ and ε are the corresponding dielectric constants, z' is the distance to the DCM2 layer, L_w is the quantum well width. The quadrupole transition matrix element Q_{xz} may be estimated from the corresponding oscillator strength per unit cell through the following identity (Moskalenko and Liberman 2002) and depends on polarization of the pumping laser field:

$$f_{xz,k_0} = \frac{4\pi m E_g}{3e^2\hbar^2} \left(\frac{a_B^W}{a}\right)^3 \left(\mathbf{z} \cdot \mathbf{k}_{0,x} \cdot Q_{x,z}\right)^2$$
$$f_{xz,\mathbf{k}_0 \| [1,1,0]} = 3.9 \times 10^{-9} \quad (A.2)$$
$$f_{xz,\mathbf{k}_0 \| [1,1,1]} = \tfrac{1}{3} 3.9 \times 10^{-9}.$$

Here the energy gap of cuprous oxide is denoted as $E_g = 2.173$ eV; $k_0 = 2.62 \times 10^5$ cm^{-1} is the resonant wavevector; a is the unit cell size; the unit vector in the pumping field polarization is $\mathbf{z}$.

Appendix B

The non-zero commutator relations for the organic and inorganic parts of the hybrid yield (Mukamel 1995):

$$\begin{gathered}\left[B_{1S}^{\dagger}, B_{1S}\right] = -1 + B_{2P}^{\dagger}B_{2P} + b^{\dagger}b;\\ \left[B_{1S}^{\dagger}, B_{2P}\right] = B_{1S}^{\dagger}B_{2P}; \qquad \left[B_{2P}^{\dagger}, B_{1S}\right] = B_{2P}^{\dagger}B_{1S}\\ \left[B_{2P}^{\dagger}, B_{2P}\right] = -1 + B_{1S}^{\dagger}B_{1S} + b^{\dagger}b;\\ \left[b^{\dagger}, B_{1S}\right] = b^{\dagger}B_{1S}; \qquad \left[b^{\dagger}, B_{2P}\right] = b^{\dagger}B_{2P}\\ \left[b^{\dagger}, b\right] = -1 + B_{2P}^{\dagger}B_{2P} + B_{1S}^{\dagger}B_{1S};\\ \left[B_{1S}^{\dagger}, b\right] = B_{1S}^{\dagger}b; \qquad \left[B_{2P}^{\dagger}, b\right] = B_{2P}^{\dagger}b.\end{gathered} \tag{B.1}$$

In the TDHF approximate factorization for the averages, the corresponding Heisenberg equations up to the second order in the creation and annihilation operators are:

$$\begin{aligned}\mathrm{i}\hbar\frac{\mathrm{d}B_{1S}^{\dagger}}{\mathrm{d}t} &= \hbar\omega_{1S}B_{1S}^{\dagger} + \Gamma_k b^{\dagger} - \mu^{\mathrm{F}}E_i B_{1S}^{\dagger}b\\ &\quad + \mu_{1S,k}E_i\left(1 - B_{2P}^{\dagger}B_{2P} - b^{\dagger}b\right)\\ &\quad - \mu_{2P}E_i B_{1S}^{\dagger}B_{2P} + \mu_{1S,2P}E_j B_{2P}^{\dagger}\\ \mathrm{i}\hbar\frac{\mathrm{d}B_{1S}}{\mathrm{d}t} &= -\hbar\omega_{1S}B_{1S} - \Gamma_k b + \mu^{\mathrm{F}}E_i^{\star}b^{\dagger}B_{1S}\\ &\quad - \mu_{1S,k}E_i^{\star}\left(1 - B_{2P}^{\dagger}B_{2P} - b^{\dagger}b\right)\\ &\quad + \mu_{2P}E_i^{\star}B_{2P}^{\dagger}B_{1S} - \mu_{1S,2P}E_j^{\star}B_{2P}\\ \mathrm{i}\hbar\frac{\mathrm{d}B_{2P}^{\dagger}}{\mathrm{d}t} &= \hbar\omega_{2P}B_{2P}^{\dagger} - \mu^{\mathrm{F}}E_i B_{2P}^{\dagger}b - \mu_{1S,k}E_i B_{2P}^{\dagger}B_{1S}\\ &\quad + \mu_{2P}E_i\left(1 - B_{1S}^{\dagger}B_{1S} - b^{\dagger}b\right) + \mu_{1S,2P}E_j B_{1S}^{\dagger}\\ \mathrm{i}\hbar\frac{\mathrm{d}B_{2P}}{\mathrm{d}t} &= -\hbar\omega_{2P}B_{2P} + \mu^{\mathrm{F}}E_i^{\star}b^{\dagger}B_{2P} + \mu_{1S,k}E_i^{\star}B_{1S}^{\dagger}B_{2P}\\ &\quad - \mu_{2P}E_i^{\star}\left(1 - B_{1S}^{\dagger}B_{1S} - b^{\dagger}b\right) - \mu_{1S,2P}E_j^{\star}B_{1S}\\ \mathrm{i}\hbar\frac{\mathrm{d}b^{\dagger}}{\mathrm{d}t} &= E^{\mathrm{F}}b^{\dagger} + \Gamma_k B_{1S}^{\dagger} + \mu^{\mathrm{F}}E_i\left(1 - B_{1S}^{\dagger}B_{1S} - B_{2P}^{\dagger}B_{2P}\right)\\ &\quad - \mu_{1S,k}E_i b^{\dagger}B_{1S} - \mu_{2P}E_i b^{\dagger}B_{2P}\\ \mathrm{i}\hbar\frac{\mathrm{d}b}{\mathrm{d}t} &= -E^{\mathrm{F}}b - \Gamma_k B_{1S} - \mu^{\mathrm{F}}E_i^{\star}\left(1 - B_{1S}^{\dagger}B_{1S} - B_{2P}^{\dagger}B_{2P}\right)\\ &\quad + \mu_{1S,k}E_i^{\star}B_{1S}^{\dagger}b + \mu_{2P}E_i^{\star}B_{2P}^{\dagger}b.\end{aligned}$$

Here we omitted the average brackets to shorten the notation. In the exact resonance between FE and WE excitons $\hbar\omega_{1S} = \hbar\omega_F$ the linear approximation is straightforward. The creation operators are $\propto \mathrm{e}^{\mathrm{i}\omega t}$ and the system above is reduced to:

$$\begin{aligned}\hbar\omega B_{1S,0}^{\dagger} &= (\hbar\omega_{1S} - \mathrm{i}\hbar\gamma)\,B_{1S,0}^{\dagger} + \Gamma_k b_0^{\dagger} + \mu_{1S,k}E_i - \hbar\omega B_{1S,0}\\ &= -(\hbar\omega_{1S} + \mathrm{i}\hbar\gamma)\,B_{1S,0} - \Gamma_k b_0 - \mu_{1S,k}E_i^{\star}\\ \hbar\omega B_{2P,0}^{\dagger} &= \hbar\omega_{2P}B_{2P,0}^{\dagger} + \mu_{2P}E_i - \hbar\omega B_{2P,0}\\ &= -\hbar\omega_{2P}B_{2P,0} - \mu_{2P}E_i^{\star}\\ \hbar\omega b_0^{\dagger} &= (\hbar\omega_{1S} - \mathrm{i}\hbar\gamma)\,b_0^{\dagger} + \Gamma_k B_{1S,0}^{\dagger} + \mu^{\mathrm{F}}E_i - \hbar\omega b_0\\ &= -(\hbar\omega_{1S} + \mathrm{i}\hbar\gamma)\,b_0 - \Gamma_k B_{1S,0} - \mu^{\mathrm{F}}E_i^{\star}.\end{aligned}$$

The system above has a solution:

$$\begin{aligned}B_{2P,0}^{\dagger} &= \frac{\mu_{2P}E_i}{\hbar\omega - \hbar\omega_{2P}}\\ B_{1S,0}^{\dagger} &= \frac{\mu_{1S}E_i\,(\hbar\omega - \hbar\omega_{1S} + \mathrm{i}\hbar\gamma) + \mu^{\mathrm{F}}\Gamma_k E_i}{(\hbar\omega - \hbar\omega_{1S} + \mathrm{i}\hbar\gamma)^2 - \Gamma_k^2}\\ b_0^{\dagger} &= \frac{\mu^{\mathrm{F}}E_i\,(\hbar\omega - \hbar\omega_{1S} + \mathrm{i}\hbar\gamma) + \mu_{1S}\Gamma_k E_i}{(\hbar\omega - \hbar\omega_{1S} + \mathrm{i}\hbar\gamma)^2 - \Gamma_k^2}.\end{aligned} \tag{B.2}$$

The SHG is due to the response to the induced polarization and is $\propto \mathrm{e}^{\mathrm{i}2\omega t}$:

$$\begin{aligned}2\hbar\omega B_{1S,1}^{\dagger} &= (\hbar\omega_{1S} - \mathrm{i}\hbar\gamma)\,B_{1S,1}^{\dagger} + \Gamma_k b_1^{\dagger} + \mu_{1S,2P}E_j B_{2P,0}^{\dagger}\\ 2\hbar\omega B_{1S,1} &= (\hbar\omega_{1S} + \mathrm{i}\hbar\gamma)\,B_{1S,1} + \Gamma_k b_1 + \mu_{1S,2P}E_j^{\star}B_{2P,0}^{\dagger}\\ 2\hbar\omega B_{2P,1}^{\dagger} &= \hbar\omega_{2P}B_{2P,1}^{\dagger} + \mu_{1S,2P}E_j B_{1S,0}^{\dagger}\\ 2\hbar\omega B_{2P,1} &= \hbar\omega_{2P}B_{2P,1} + \mu_{1S,2P}E_j^{\star}B_{1S,0}^{\dagger}\\ 2\hbar\omega b_1^{\dagger} &= (\hbar\omega_{1S} - \mathrm{i}\hbar\gamma)\,b_1^{\dagger} + \Gamma_k B_{1S,1}^{\dagger}\\ 2\hbar\omega b_1 &= (\hbar\omega_{1S} + \mathrm{i}\hbar\gamma)\,b_1 + \Gamma_k B_{1S,1}.\end{aligned}$$

The system has a solution:

$$\begin{aligned}B_{2P,1}^{\dagger} &= \frac{\mu_{1S,2P}E_j B_{1S,0}^{\dagger}}{2\hbar\omega - \hbar\omega_{2P}}\\ B_{1S,1}^{\dagger} &= \frac{\mu_{1S,2P}E_j\,(2\hbar\omega - \hbar\omega_{1S} + \mathrm{i}\hbar\gamma)\,B_{2P,0}^{\dagger}}{(2\hbar\omega - \hbar\omega_{1S} + \mathrm{i}\hbar\gamma)^2 - \Gamma_k^2}\\ b_1^{\dagger} &= \frac{\mu_{1S,2P}E_j\Gamma_k B_{2P,0}^{\dagger}}{(2\hbar\omega - \hbar\omega_{1S} + \mathrm{i}\hbar\gamma)^2 - \Gamma_k^2}.\end{aligned} \tag{B.3}$$

These solutions are implemented in the main text to calculate the linear and nonlinear responses of the hybrid.

References

Agranovich V, Basko D, Rocca G L and Bassani F 1998 *J. Phys.: Condens. Matter* **13** 9369

Artoni M, Carusotto I, La Rocca G and Bassani F 2002 *J. Opt. B.: Quantum Semiclass. Opt.* **4** S345

Atanasov R, Bassani F and Agranovich V 1994 *Phys. Rev.* B **50** 7809

Bloembergen N 1965 *Nonlinear Optics* (New York: Benjamin)

Bulovic V, Deshpande R and Forrest S 1999 *Chem. Phys. Lett.* **308** 317

Dasbach G 2004 *Phys. Rev.* B **70** 121202

Elliott R J 1961 *Phys. Rev.* **124** 340

Engelmann A, Yudson V I and Reineker P 1998 *Phys. Rev.* B **57** 1784

Frohlich D, Dasbach G, Hogersthal G B, Bayer M, Kliebera R, Sutera D and Stolzb H 2005 *Solid State Commun.* **134** 139

Gao Y, Birman J, Huong N and Potasek M 2004 *J. Appl. Phys.* **96** 1

Haueisen D and Mahr H 1973 *Phys. Rev.* B **8** 734

Huong N Q and Birman J L 2000 *Phys. Rev.* B **61** 13131

Huong N Q and Birman J L 2003 *Phys. Rev.* B **67** 075313

Kishida H, Hasegawa T, Iwasa Y, Koda T, Tokura Y, Tachibana H, Matsumoto M, Wada S, Lay T and Tashiro H 1994 *Phys. Rev.* B **50** 7786
Madigan C and Bulovic V 2003 *Phys. Rev. Lett.* **91** 247403
Madigan C and Bulovic V 2004 *Bringing Materials Research Together*
Moskalenko S and Liberman M 2002 *Phys. Rev.* B **65** 064303
Mukamel S 1995 *Principles of Nonlinear Optical Spectroscopy* (New York: Oxford Press)
Roslyak O and Birman J 2007a *Solid State Commun.* **143** 487
Roslyak O and Birman J L 2007b *Phys. Rev.* B **75** 245309
Shen M, Koyama S, Saito M, Goto T and Kuroda N 1996 *Phys. Rev.* B **53** 13477